Dear Prof. Gerbi,

We appreciate your helpful comments. Here we present our responses to the comments. Our responses are in black, while your comments are in blue. We will make necessary revisions to address the questions.

This is a very valuable study to provide additional constraints on the crystallographic development of Ice Ih. As the authors note, the ice fabric plays a significant role in glacier and ice sheet mechanics, so being able to predict and explain fabric development provides a much stronger grounding for describing and modeling ice flow.

I particularly appreciate the authors explaining their experimental steps in such detail – it makes it easy for the reader to follow and understand the strengths of their approach. In addition, the primary conclusion of this study, namely the persistence of a secondary, albeit weak, c-axis cluster even at high shear strain, appears quite robust. I offer my suggestions below in the spirit of making the analysis more transparent, and thus easier to compare with other work.

Sensitivity. Line 175 and following suggest that all calculations related to the fabric use all orientation data. However, determining which pixels are labeled as ice vs graphite seems to have been a non-trivial exercise. Did the authors perform any sensitivity to evaluate how their processing algorithm may affect the final orientation or other datasets?

This is a good suggestion. To clarify, the data used to calculate the CPO for all orientation with a 30-μm step size do not involve extrapolation of unindexed points. We have restructured the section, so that the analysis of CPO (using 30-μm step size) and grain size (using 15-μm step size) are separated. For the data with a 15-μm step size, we did extrapolate unindexed points, incorporating EDS data in the process. In this extrapolation, the intensity of the graphite signal (greater than 1) is a crucial parameter. We performed sensitivity tests using different thresholds for the graphite signal intensity (1, 2, 4) to assess the impact of this extrapolation on microstructural features, such as grain size. The table below shows the effect of different thresholds for the graphite signal intensity on shape preferred orientation (SPO) and grain size after extrapolation.

The table demonstrates that the choice of signal intensity threshold has a slightly effect on the microstructural analysis. As the threshold increases, the SPO angle

slightly decreases, while grain size slightly increases. However, the magnitude of these changes is subtle, which may be attributed to differences in the index rate. Since unindexed areas are assigned to surrounding grains during the grain reconstruction process, the index rate can influence the final results after reconstruction. Overall, the threshold selection follows a consistent trend across the samples. As long as all samples were processed using the same threshold, our data are comparable between each other.

Table S1. The effect of different thresholds for EDS data on SPO and grain size.

	Threshold of signal	undeformed	33_1p	19_2p	19_3p	21_4p	34_5p	38_6p
SPO (°)	1		32	12	14	11	17	9
	2		26	10	12	10	14	8
	4		22	6	10		13	8
grain size (μm)	1	140	180	167	211	139	155	143
	2	154	195	186	222	137	168	149
	4	162	207	203	234		180	153

As part of this, I would like to see an explanation of why the EDS and EBSD data were collected separately at different step sizes, as I would have thought that the hardware and software would allow for simultaneous collection.

Theoretically, the Aztech software allows simultaneous collection of EDS and EBSD data. However, we meet a technical challenge that EDS and EBSD require different acceleration voltages. Ice EBSD requires 30kV, but to get good quality EDS data for graphite, lower voltages (~15kV) are needed to EDS. Consequently, we need to scan twice using different voltages for EBSD and EDS. Meanwhile, since EDS was done separately, we tried to collect EDS data at a higher resolution, that is why the pixel of EDS is smaller than the step size of EBSD.

With some work, I think I can understand which figures and interpretations rely on the 15um vs 30um step size EBSD data. At the same time, I think that could be more clearly explained in the text.

Thank you for pointing this out. We have restructured the section, so that the analysis of CPO (using 30-μm step size) and grain size (using 15-μm step size) are in two subsections now.

line 157-158:

2.4 Analysis of microstructure

“Data with a 15-μm step size were combined with EDS data to identify unindexed

points, which were then used to analyze grain size, aspect ratio, and shape preferred orientations."

Section 2.5 Analysis of crystallographic orientations

"Orientation distributions were generated from the complete set of raw EBSD data with 30 μm step size using the MTEX toolbox in MATLAB (Bachmann et al, 2010; Mainprice et al, 2015). To quantify the strength of the CPOs, both the J-index (Bunge, 1982) and the M-index (Skemer et al, 2005) were used."

Additionally, we also added the information on step size in the caption.

"Figure 5. Microstructural analyses of an undeformed ice samples, using EBSD data with a 15-μm step size."

"Figure 8. Crystallographic fabric strength as a function of strain, based on EBSD data with a 30-μm step size."

"Figure 9. Aspect ratio of clusters as a function of strain, based on EBSD data with a 30-μm step size."

"Figure 10. Microstructure results for all deformed samples, based on EBSD data with a 15-μm step size."

Number of data points. I may have missed it, but I didn't see a total of the number of datapoints used in the orientation data analysis. I suggest adding that value to perhaps Figure 7 or Table 1.

Reply: Thank you for the suggestions. We have added it to Table 1.

Table 1. Summary of experiments. ε' is nominal equivalent strain, φ is the angle between the two clusters.

Sample	Graphite fraction	Passes	Load (Kg)	Length (mm)	ε'	Part for analysis	points of EBSD data	area(mm*mm)	φ
ECAP_33	2.1wt.% (0.9 vol.%)	1	42.5	110	0.6	ECAP_33_1P	144045	14.85*8.73	50◦
ECAP_19	3.6wt.% (1.5 vol.%)	1	42.5	98	0.6				
		2	37.5	100*	1.2	ECAP_19_2P	99099	12.87*6.93	55◦
		3	37.5	50	1.8	ECAP_19_3P	104550	12.75*7.38	50◦
ECAP_21	1.8wt.% (0.8 vol.%)	1	42.5	110	0.6				
		2	37.5	105	1.2				
		3	37.5	93	1.8				
		4	32.5	85	2.4	ECAP_21_4P	108035	15.81*6.15	45◦
ECAP_34	2.6wt.% (1.1 vol.%)	1	42.5	107	0.6				

		2	32.5	99	1.2				
		3	32.5	95	1.8				
		4	32.5	85	2.4				
		5	32.5	65	3	ECAP_34_5P	112892	13.86*7.97	60◦
ECAP_38	2.2wt.% (0.9 vol.%)	1	42.5	105	0.6				
		2	32.5	100	1.2				
		3	32.5	95	1.8				
		4	32.5	95	2.4				
		5	32.5	92	3				
		6	32.5	94	3.6	ECAP_38_6P	161100	16.11*9	55◦

Line 219: when discussing stress, presumably you mean differential, deviatoric, or shear stress? Please clarify.

Thank you for pointing this out. In most cases, we mean shear stress. For deviatoric stress and equivalent stress, we always write them out. Based on comments from Reviewer 1, this sentence has been deleted. And we have changed “stress” to “shear stress” in the next paragraph.

Line 257 refers to larger analysis areas used than presented in the paper. I would appreciate seeing the full maps (in appendix), as they help the reader evaluate heterogeneity. Similarly, for Figure 10, I would find it useful to indicate that the histograms and rose diagrams use larger datasets than shown if that is accurate.

Reply: Thank you very much for your suggestion, we have added the complete map in the supplementary. The supplementary figures are illustrated as follows.

ECAP_33_1p

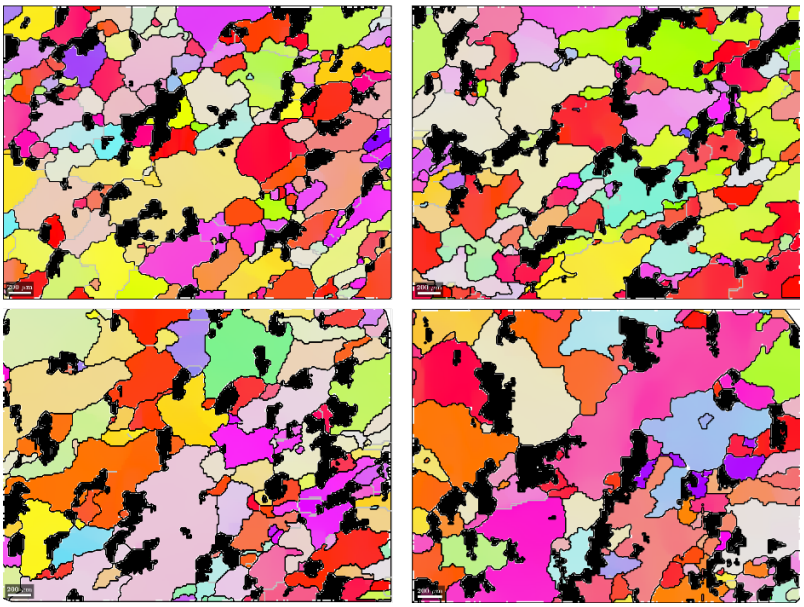

ECAP_19_2p

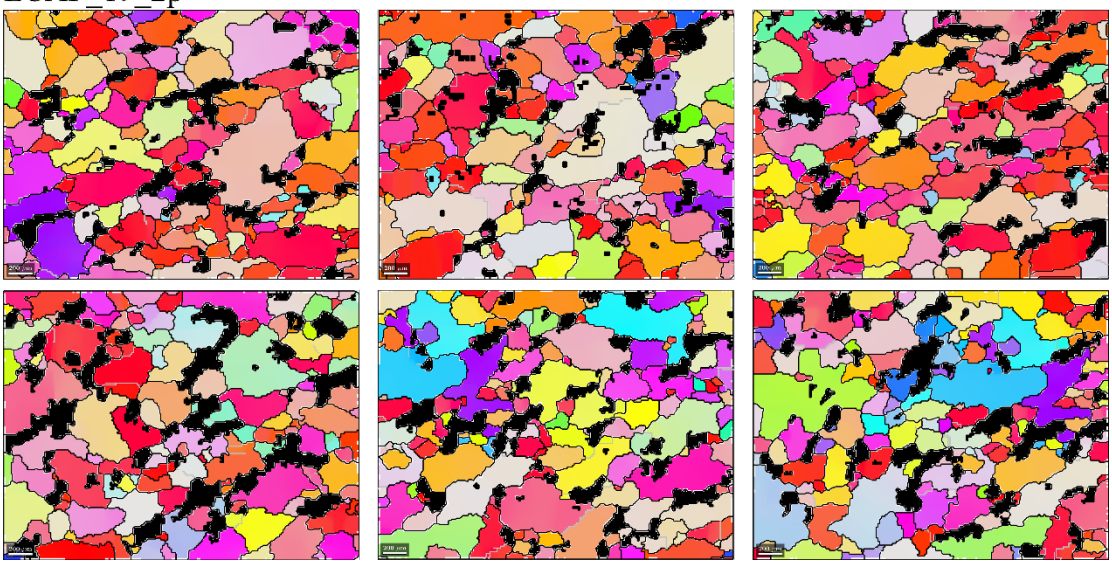

ECAP_19_3p

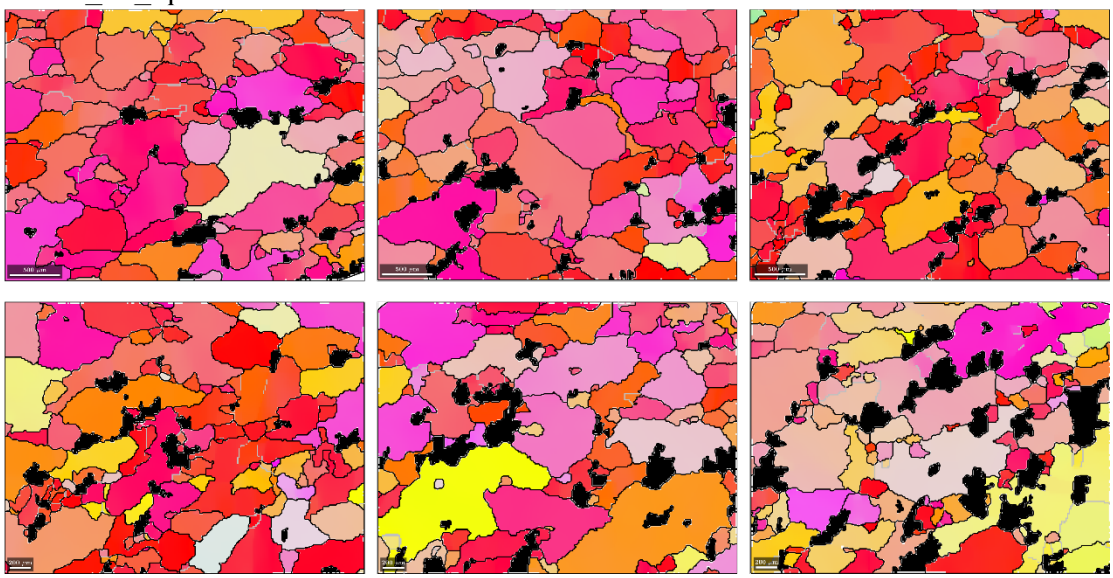

ECAP_21_4p

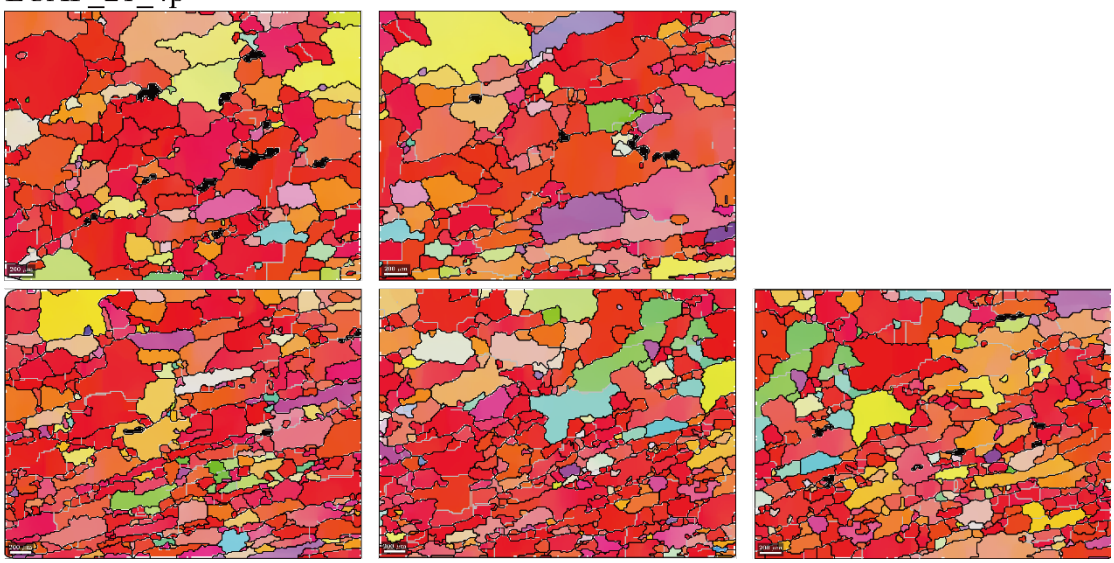

ECAP_34_5p

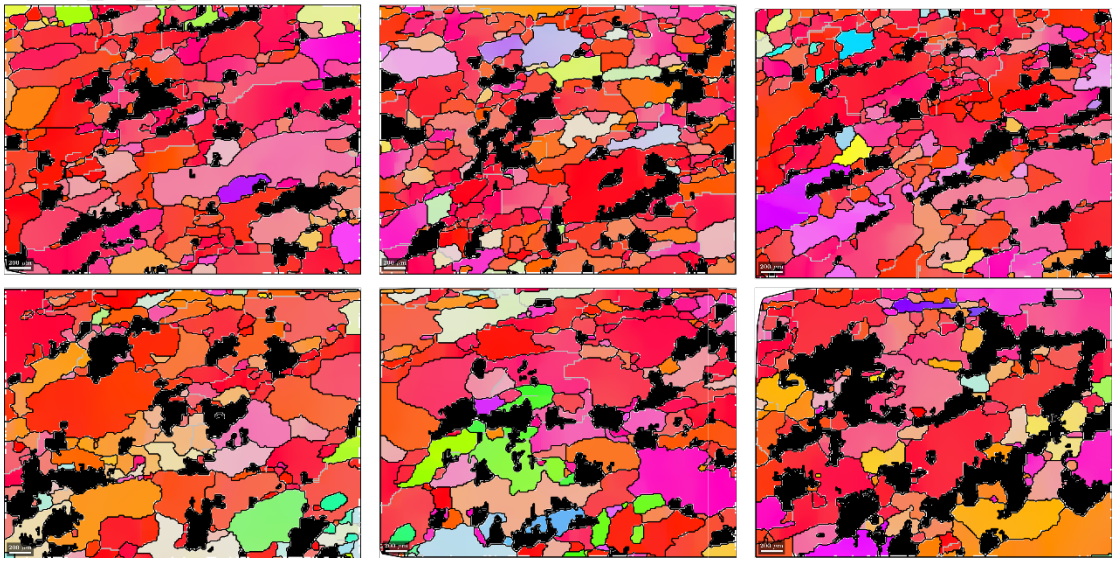

ECAP_38_6p

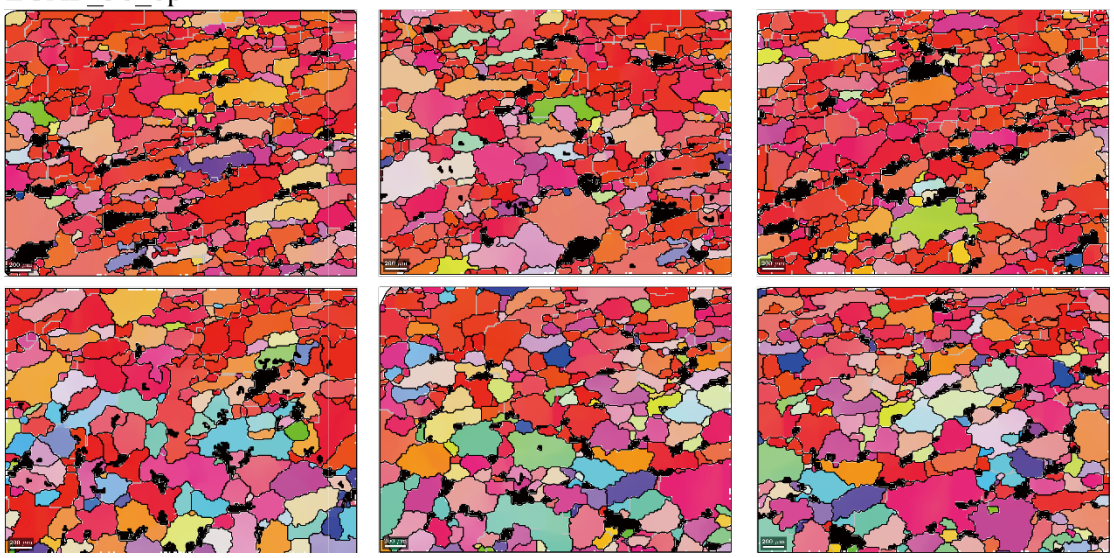

For the reader to best appreciate the comparison of the experimental data with the modeled data, I suggest adding a section to Results to present the SpecCAF calculations. That way, the model results can stand somewhat independently for the later comparison.

We thank the reviewer for the suggestion. We have added a new subsection in the Results section.

“Section 3.5 Numerical modeling

The SpecCAF model requires deformation, temperature, and initial CPO as inputs. The model was run in simple shear, as the ECAP mostly results in simple shear. The

model was also run at -5°C, same as the experimental condition. The initial condition for CPO was set to isotropic, similar to our initial samples. The model was also run with the parameter β controlling the effect of GBM, reduced to different fractions (k) of the value Richards et al. (2021) found for T = −5°C (β0). The output of the modeling was the predicted angle between the c-axis clusters, φ, plotted alongside the experimental results in Fig. 11. The value of φ decreases with increasing shear strain. At a given strain, the value of φ decreases with decreasing β. At higher values of β (0.6 --- 1β0), φ decreases from over 80° to ~70° as shear strains increases to 1 and stays roughly constant at larger strains. At lower values of β (0.2 --- 0.5β0), the curves of φ terminate at different strains. This termination means the model cannot identify a secondary c-axis cluster, and the CPO is characterized by a single cluster. At β = 0.5β0, φ rapidly decreases from ~80° to around 60° as shear strain increases to 1, and gradually decreases at larger strains until the secondary cluster disappears at a shear strain of ~2.6. At β = 0.4β0 and 0.2β0, φ rapidly decreases to ~50° and ~30°, when the secondary cluster disappears at shear strains of ~1.3 and ~0.5, respectively. The curve of φ at β = 0.6β0 was found to closely match the experimental results in this study. The modelled CPOs at this value of β are illustrated in Fig 12."

Lines 182-3 and Figure 7d. It isn't clear to me how the data that lie off the profile line are used in the production of the histogram. Are all data projected onto the profile line? Or does the histogram include only a subset within a certain angular distance from the profile line? This may be explained in Qi et al. (2019), but a short review here (could also be in the appendix) would be helpful.

Reply: "We adopted a method similar to that of Fig. 2 in Qi et al. (2019). As illustrated in Supplementary Fig. S2(b), pole figures were generated using a lower hemisphere equal-area projection, with the shear plane (green circle) oriented perpendicular to the page. In the stereonets, angles ranging from 0 to 180° were defined on the shear plane. At a given angle, two semicircles with 5◦ between them (orange circle) were drawn perpendicular to the page. The number of data points falling between these semicircles was counted, normalized, and plotted as the frequency for each angle in a histogram. The angle φ was defined as the angle between the two peaks in the histogram (Supplementary Fig. S2(c))."

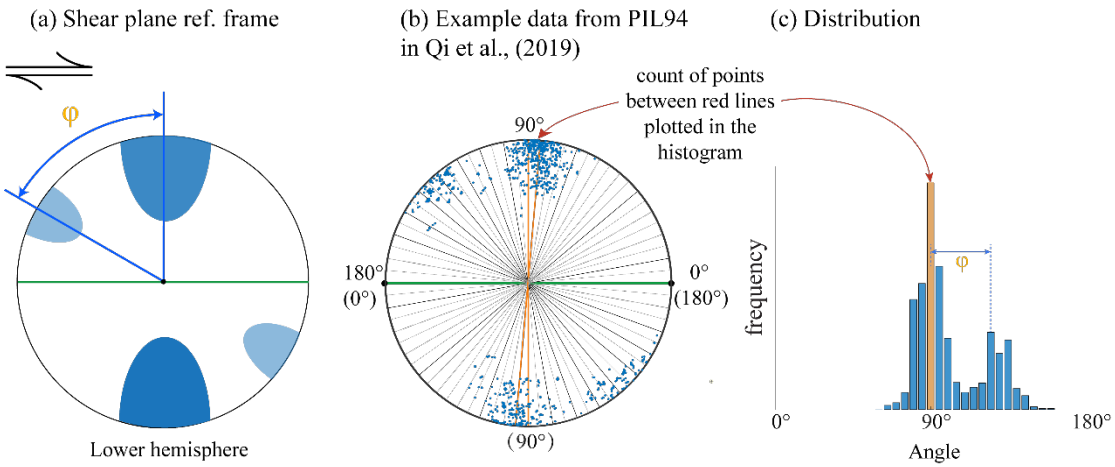

"Supplementary Figure S2. (a) Typical two-cluster distribution of *c* axes on stereonets within the shear plane reference frame. (b) A schematic illustration explaining the method used to quantify the distribution of *c* axes. (c) A histogram of *c* axes plotted in a histogram, illustrating the angle φ between the two clusters of *c* axes."

In a similar vein, how do the authors define the boundaries of the clusters to calculate the ratio plotted in Figure 8c?

Reply: The ratio between the two clusters shown in Fig. 8c was determined by comparing the peak values of the distribution frequencies for each cluster, specifically at the 5° interval. We have added a sentence explaining this in the paragraph on φ. See the reply to the previous comment.

Section 4.5. Another natural dataset for comparison is from the temperate Jarvis Glacier in Alaska [Gerbi C et al. (2021). Microstructures in a shear margin: Jarvis Glacier, Alaska. Journal of Glaciology 67(266), 1163–1176. https://doi.org/10.1017/jog.2021.62]. The results paint a different picture than the experimental results here, but the conditions are also quite different, thus providing some assessment of the applicability of the present work.

We apologize for overlooking this research. We have now included the relevant information in Section 4.5.

"Gerbi et al., (2021) investigated the microstructure of the lateral shear margins of a temperate glacier, Jarvis Glacier. Despite the fabric being relatively weak due to high water content, and short flow distance, c axes are slightly more concentrated in regions closer to the margin where strain is larger. However, without azimuth angles, it is not possible to determine the orientation of these samples relative to the shear

plane."

Line 435: The authors suggest that the changing intensity of orientations clusters may relate to the number of grains in particular orientations. Could it instead (or also) be that the sizes of the grains change such that instead of having fewer grains in low-Schmid-factor orientations, it is just that these grains are smaller? This comment is based on the presumption that the data presented are all pixels as suggested in Figure 7, rather than one-point-per-grain.

This is a reasonable concern. First, let me clarify that our CPO analysis is based on EBSD data with a 30-μm step size. Our goal is to cover a large area in limited time, so that the data is more representative for the sample. Considering the grain size, there are probably 4-6 points across a grain. Grain reconstruction based on such data did not give us good quality.

Second, due to the influence of graphite on the EBSD data, the graphite-rich regions are not indexed. Without combining EDS+EBSD data together, we found the noise reduction process in channel5 will artificially enlarge some grains, and MTEX are not able to process grains for that data. So, we cannot reconstruct grains to create a pole figure for each individual grain.

However, based on our orientation results and grain sizes reconstructed with a 15 μm step size (Figures 10a and 10b in the article), grain-size distributions in 4P–6P samples can be well fit by a log-normal distribution. This suggests that there are not a group of small grains.

Additionally, Qi et al. (2019) reported that the pole figure from full orientation data (Figure 4c in Qi et al. (2019)) exhibits stronger secondary clustering compared to the one-point-per-grain pole figure (Figure 4b in Qi et al. (2019)). This observation suggests that low-Schmid-factor grains are fewer in number but often have larger grain areas.

In the discussion, I suggest adding two subsections. One is for the limitations of these experiments: that is, under which natural conditions do the authors think these experiments apply? The second relates to rheological implications. The introduction opens with reference to the value of this work for rheology. I would find it quite valuable for the authors to reflect on how their work impacts the evolution of the mechanical properties of sheared ice.

We thank the suggestions. Now a subsection "4.8 Implications to natural ice" is added.

“As ice is a highly anisotropic material, once formed, the CPO has significant influences on the mechanical strength of ice, and thus, models of the flow of natural ice often rely on applying an anisotropy factor to the laboratory-derived flow laws (Pimienta et al., 1987). Although the models using an anisotropy factor obtained from historic observations generally predict the right magnitude of glacial flow rates, Azuma’s CPO-only flow law (Azuma, 1994) best describes the strength evolution as strain increases (Fan et al., 2021). The anisotropic factor in Azuma’s CPO-only flow law is not based on phenomenological data but calculated from the orientation data of *c* axes. Thus, this study and many previous studies focusing on the CPO development in ice aim to understand the physical processes that controls the evolution of c-axis orientation during deformation, and thus, to better constrain the anisotropy factor and predict the glacial flow rates, especially for ice-stream margins, where shear deformation is severe.

One important result from the observations of this study is that the secondary *c*-axis cluster remains its orientation and weakens with increasing strain. This result changes our previous intuitive hypothesis and provides different values of anisotropy factors at strains when the *c*-axis fabric is evolving from double clusters to a single cluster. Such fabric evolution could occur at regions not too far away from the dome, where the shear deformation just starts, and possibly at the upstream regions of ice-stream margins, where the shear plane changes from horizontal to vertical, and the fabric has to evolve accordingly. However, it is necessary to note that the laboratory observed microstructures and their evolutions are obtained at strain rates and stresses larger than those in natural ice bodies. The contribution from rotation recrystallization in natural ice could be weaker, as stresses are smaller. Moreover, natural ice is usually impure. Insoluble particles and air bubbles could accumulate along grain boundaries and reduce grain boundary mobility and inhibit GBM, which possibly also occurred in the experiments of this study. The effects of the two mechanisms can only be qualitatively discussed for natural conditions. The microstructural processes observed in laboratory experiments provides good constrains on models and simulations (e.g., Richards et al., 2021; Hunter et al., 2022), which could extrapolate laboratory results to natural ice.”